Supporting Information

Carboxamide and carbamate substituted π-conjugated polymers: the effect of hydrogen bonding on photovoltaic properties

Wei Yang,[a] Dayong Zhang,[b] Junsheng Yu*[b] and Qing Zhang*[a]

[a]*Shanghai Key Laboratory of Electrical Insulation and Thermal Aging, School of Chemistry and Chemical Engineering, Shanghai Jiaotong University, 800 Dongchuan Road, Shanghai, China*
[b]*State Key Laboratory of Electronic Thin Films and Integrated Devices, School of Optoelectronic Science and Engineering, University of Electronic Science and Technology of China (UESTC), Chengdu 610054, P. R. China*

1. NMR and Mass Spectra of Compounds

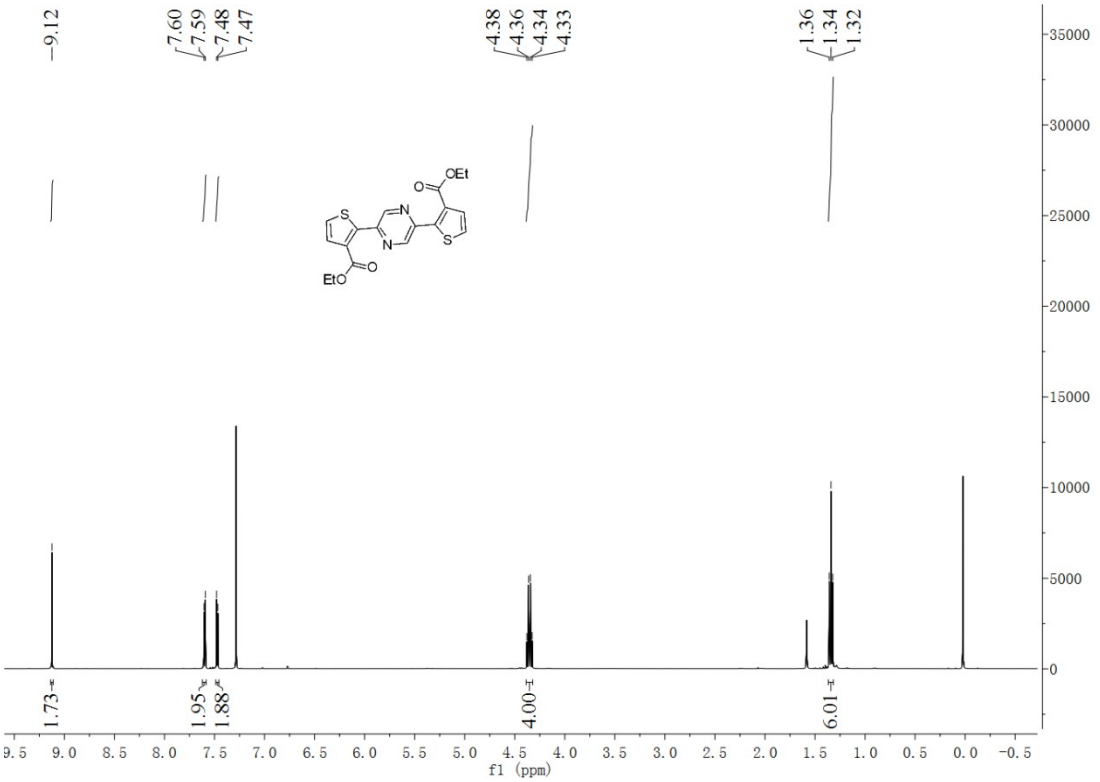

Figure S1 ^{1}H NMR spectrum of **2** in $CDCl_3$

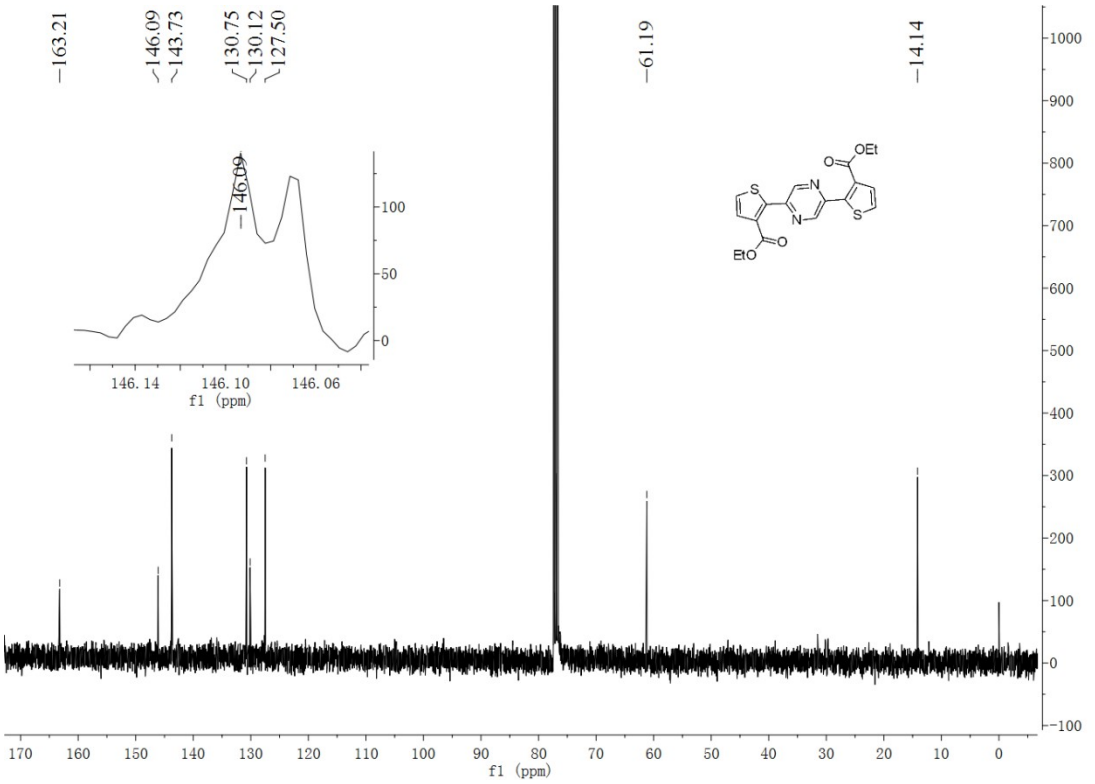

Figure S2 ^{13}C NMR spectrum of **2** in $CDCl_3$

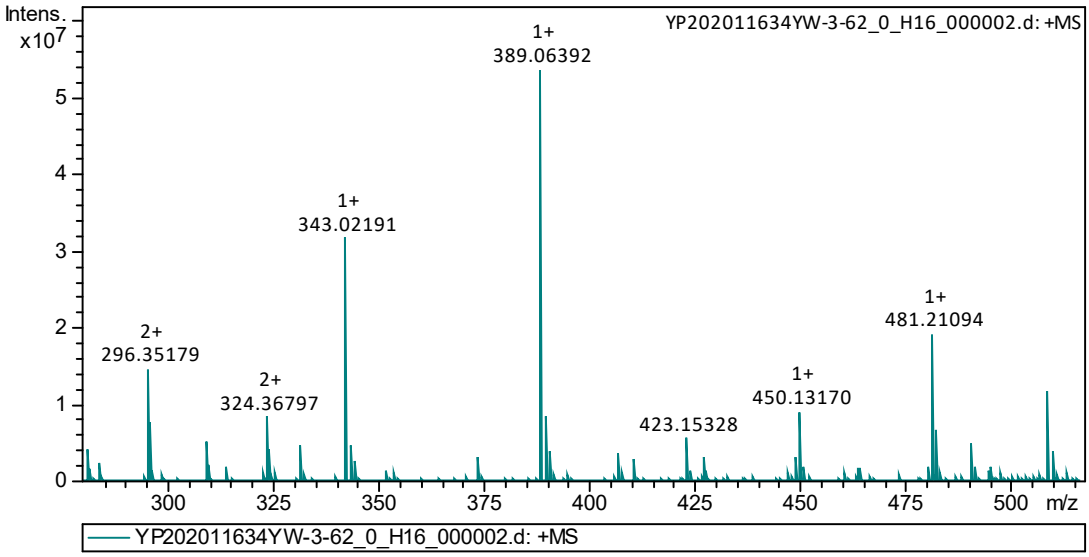

Figure S3 High-resolution MALDI-TOF MS spectrum of **2**

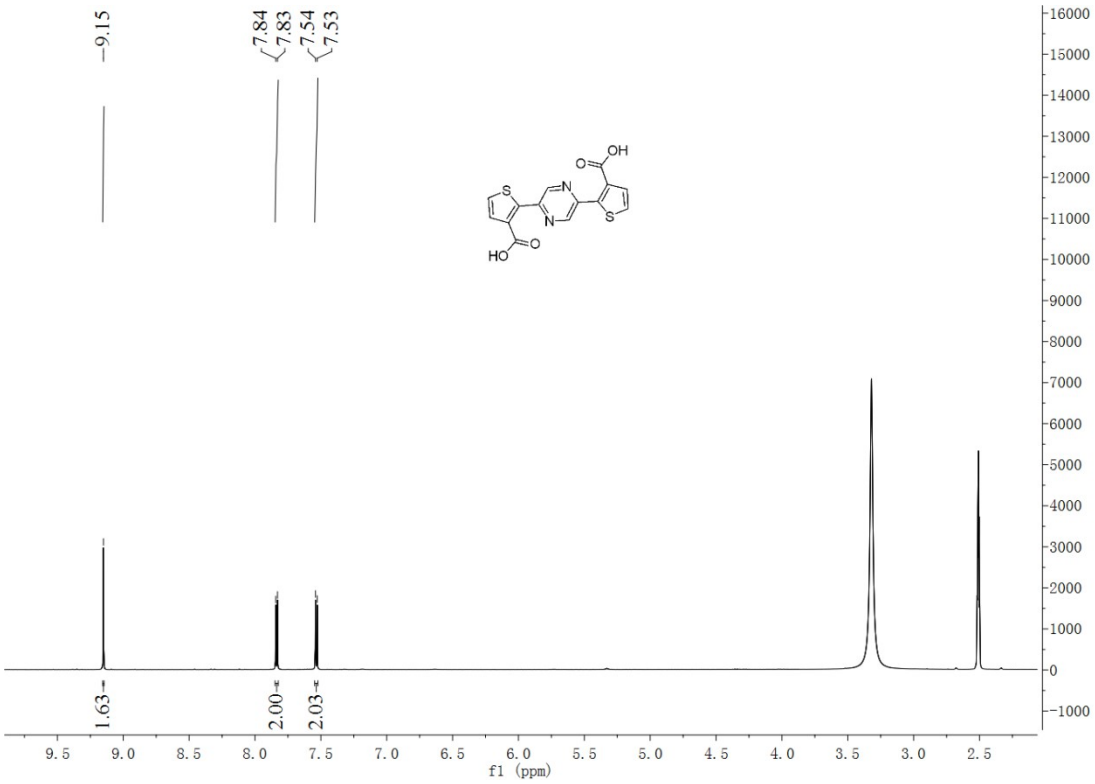

Figure S4 ^{1}H NMR spectrum of **3** in DMSO.

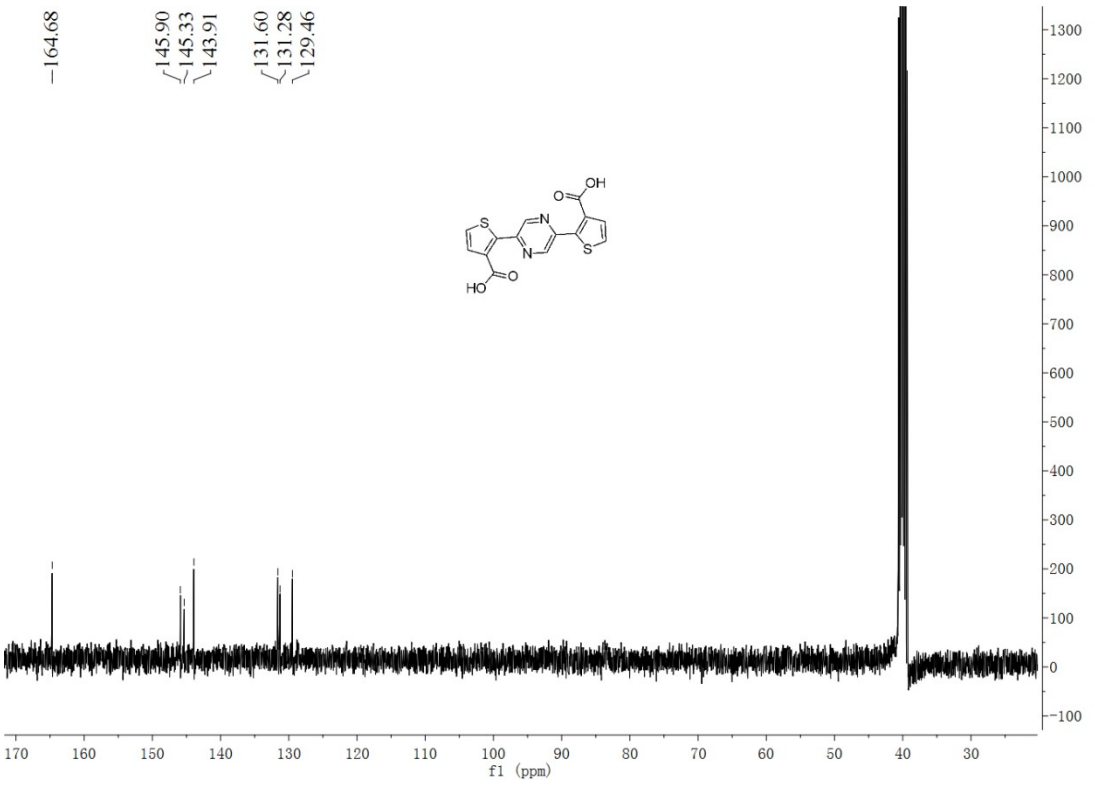

Figure S5 ^{13}C NMR spectrum of **3** in DMSO

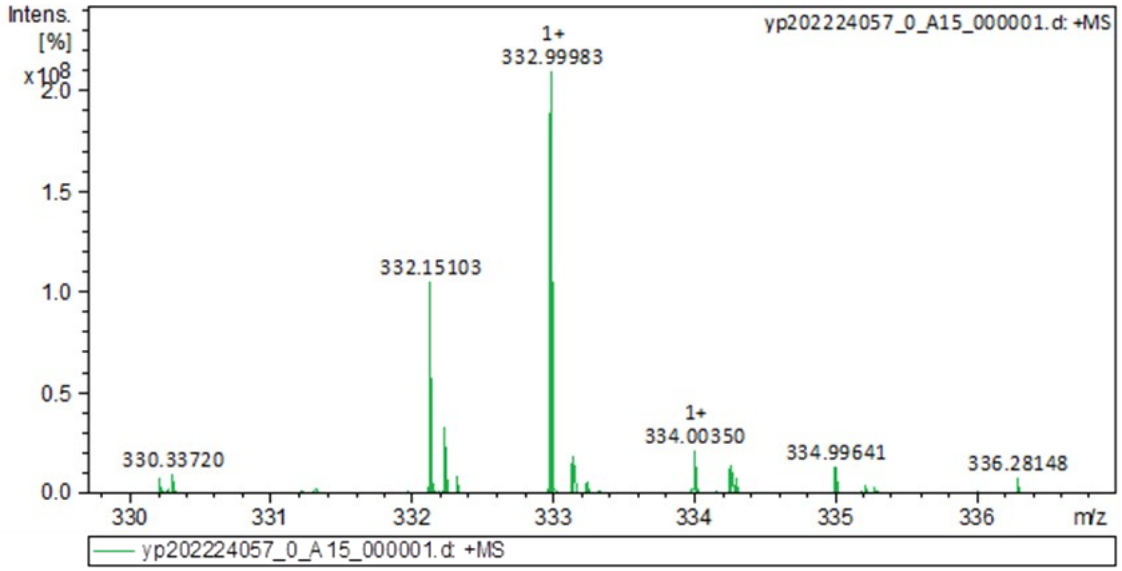

Figure S6 High-resolution MALDI-TOF MS spectrum of **3**

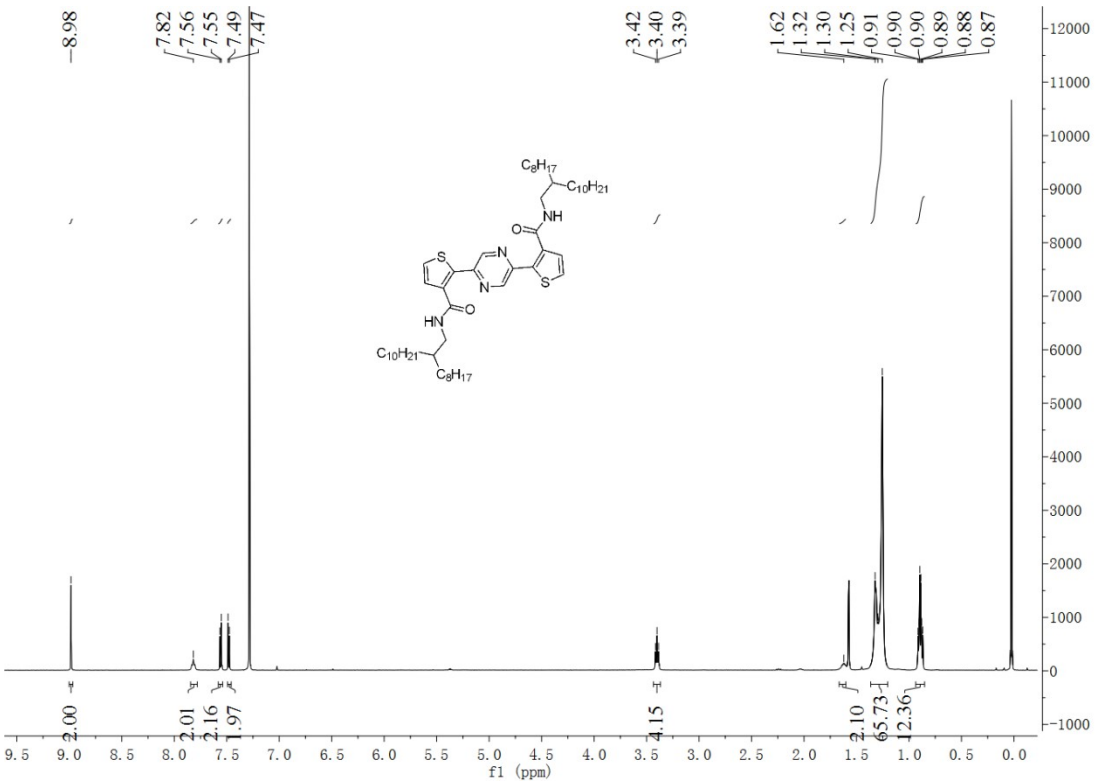

Figure S7 ^{1}H NMR spectrum of **4** in $CDCl_3$.

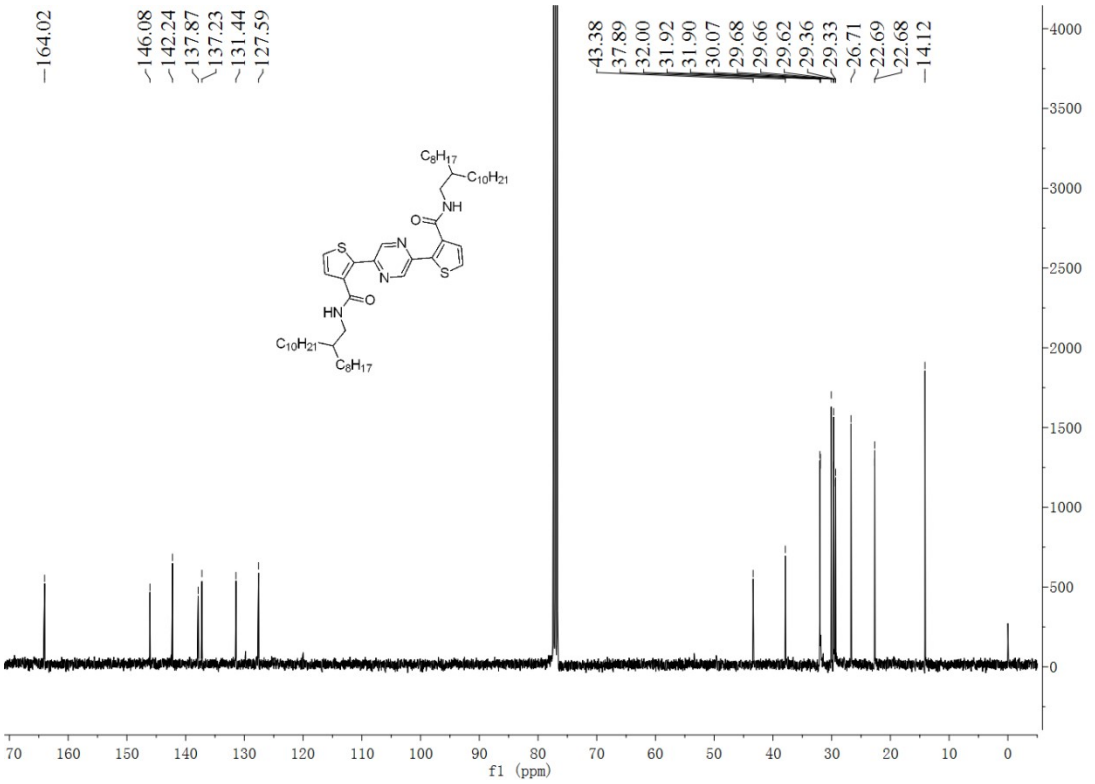

Figure S8 ^{13}C NMR spectrum of **4** in $CDCl_3$

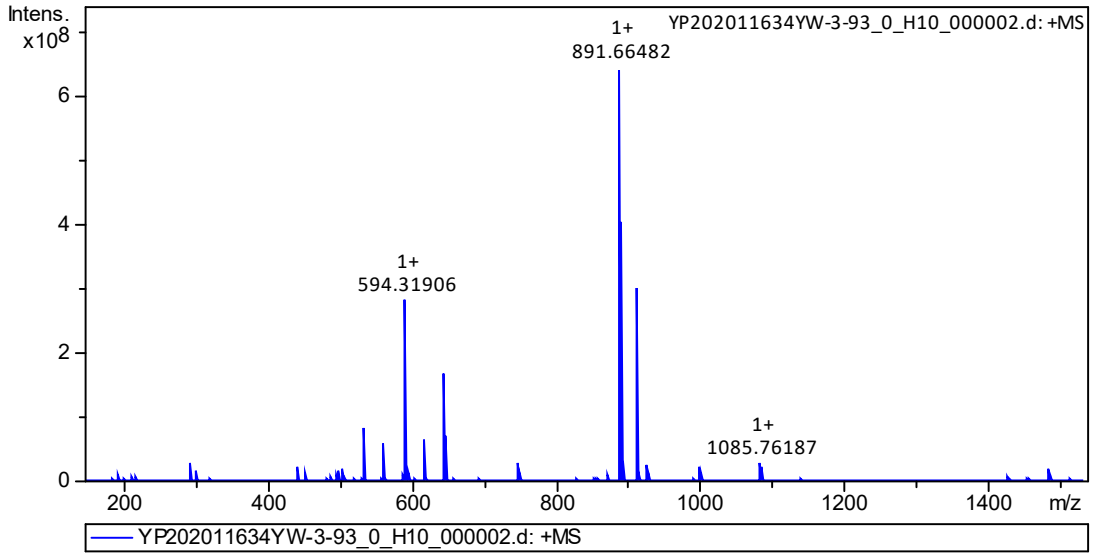

Figure S9 High-resolution MALDI-TOF MS spectrum of **4**

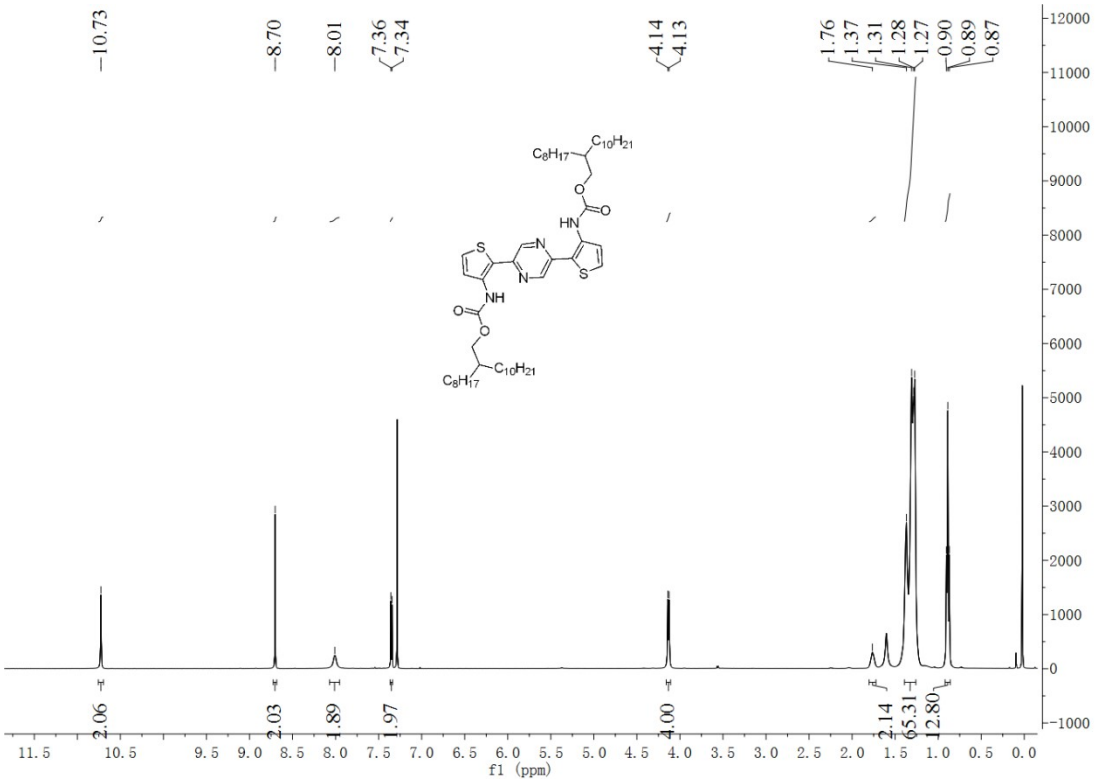

Figure S10 ^{1}H NMR spectrum of **5** in $CDCl_3$.

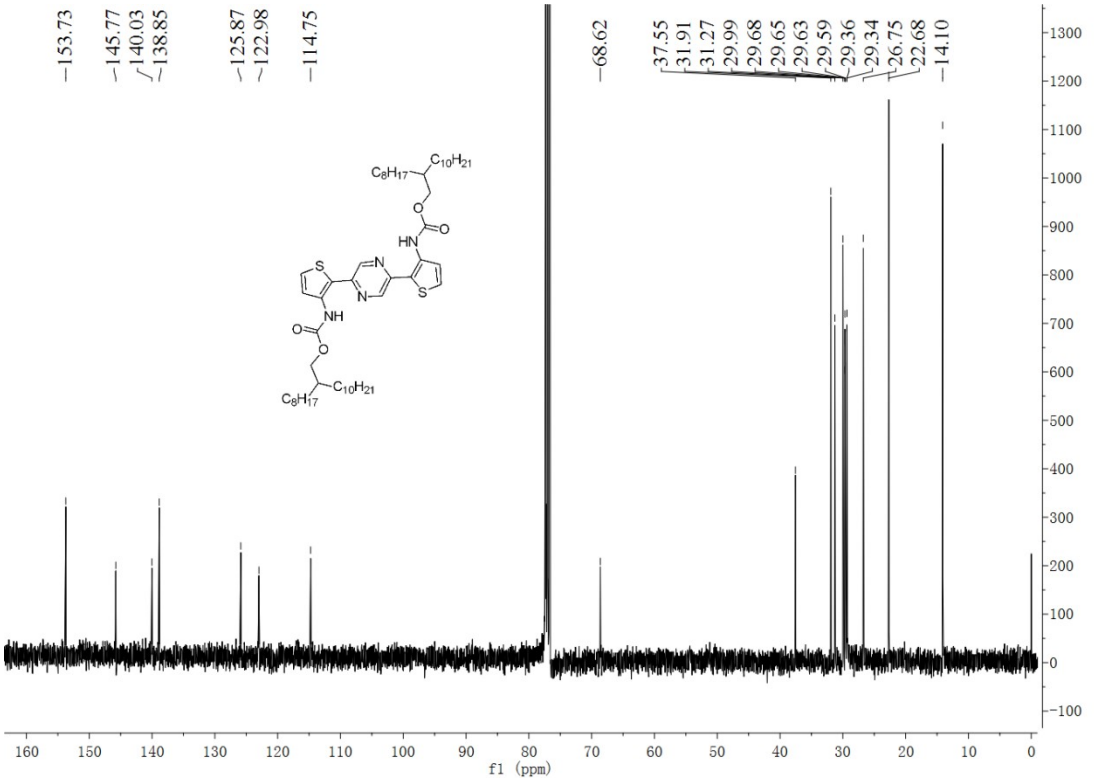

Figure S11 ^{13}C NMR spectrum of **5** in $CDCl_3$

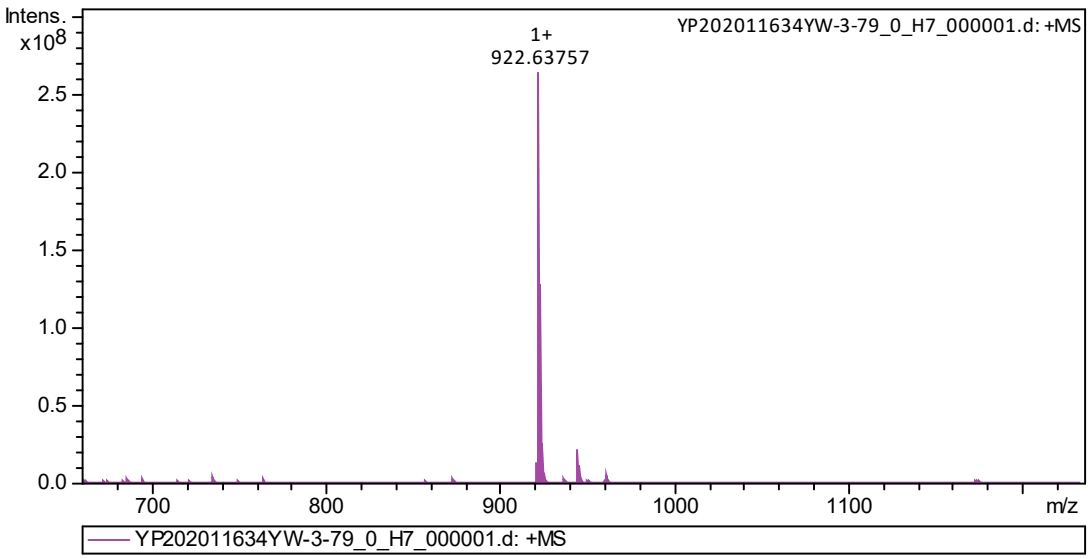

Figure S12 High-resolution MALDI-TOF MS spectrum of **5**

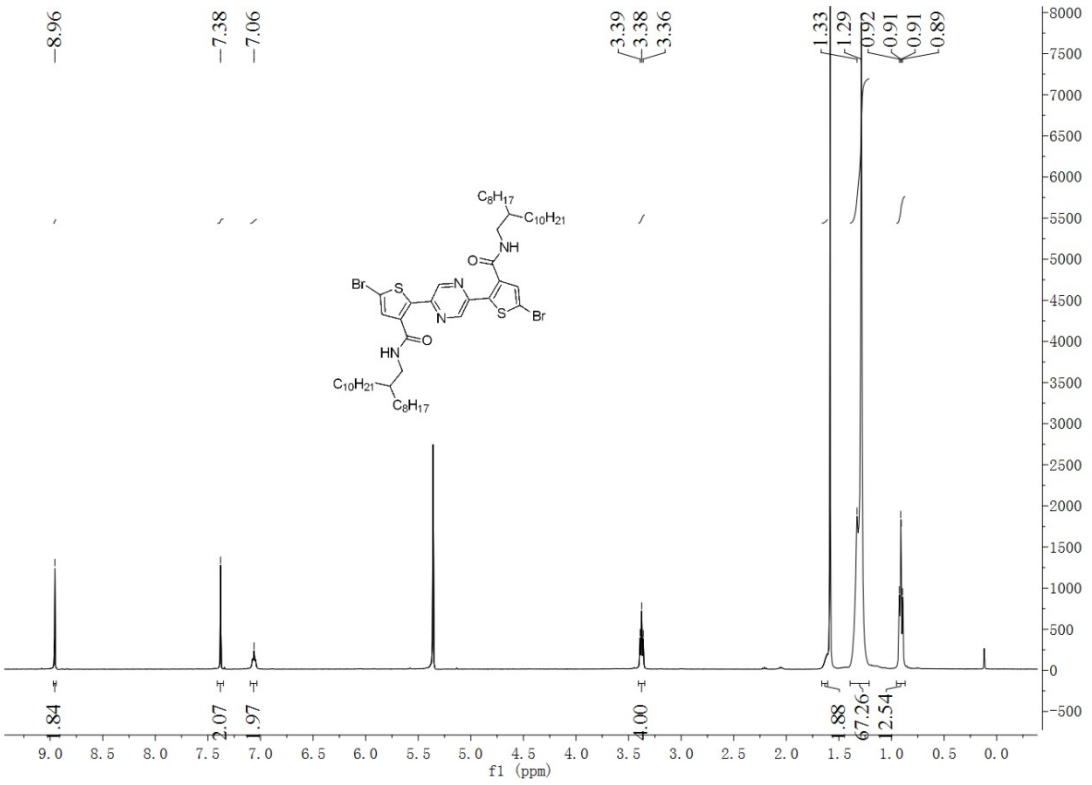

Figure S13 ^{1}H NMR spectrum of **6** in $CDCl_3$.

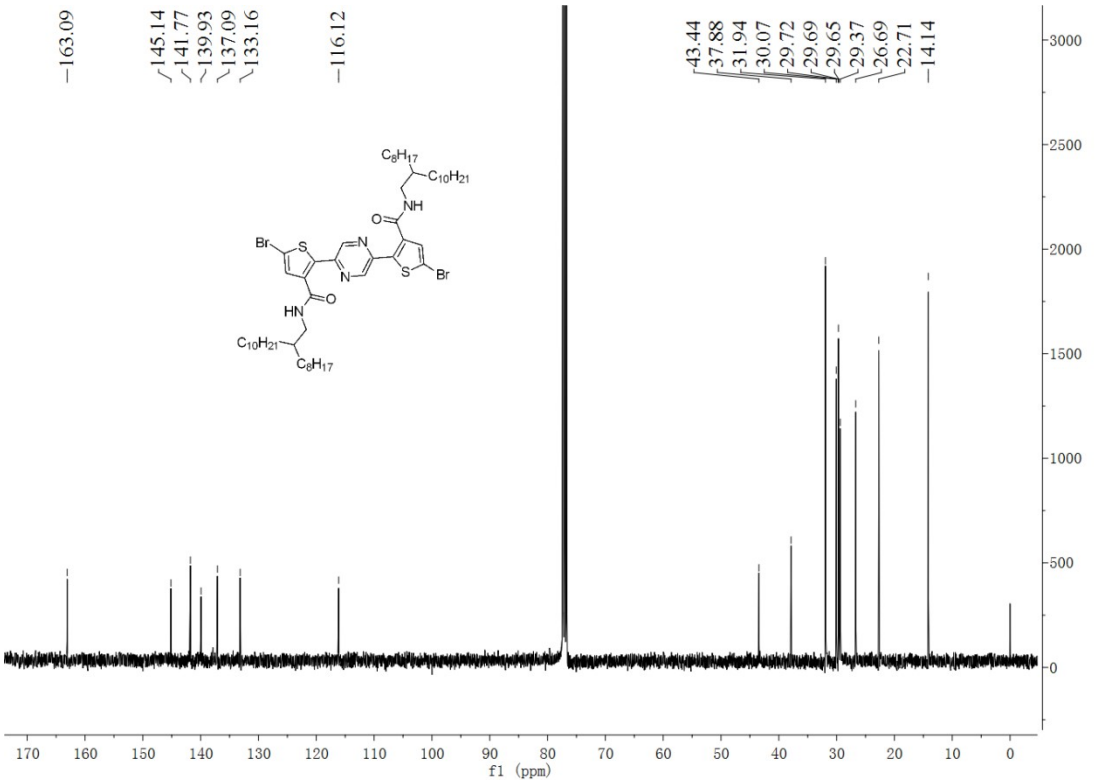

Figure S14 ^{13}C NMR spectrum of **6** in $CDCl_3$

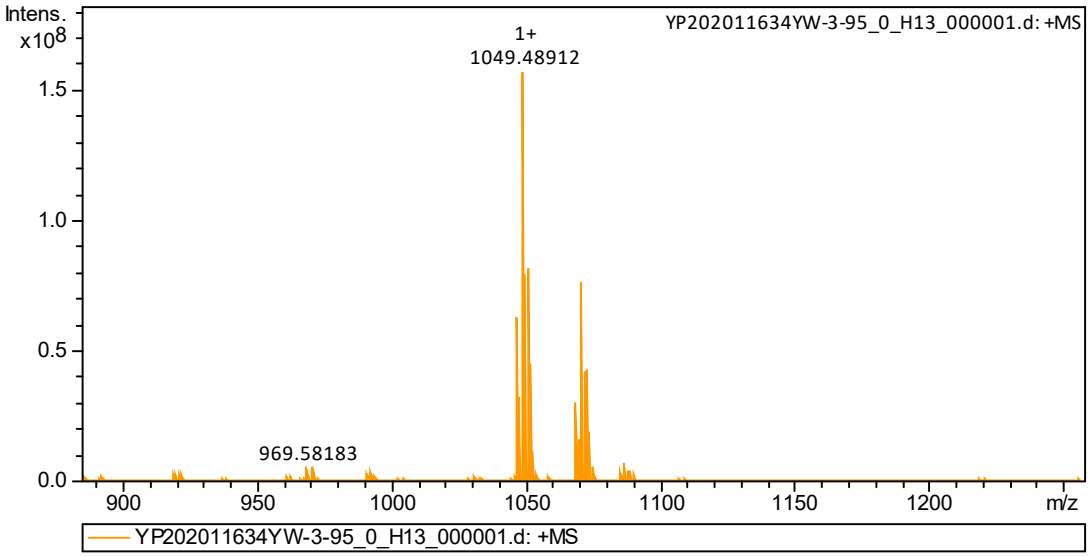

Figure S15 High-resolution MALDI-TOF MS spectrum of **6**

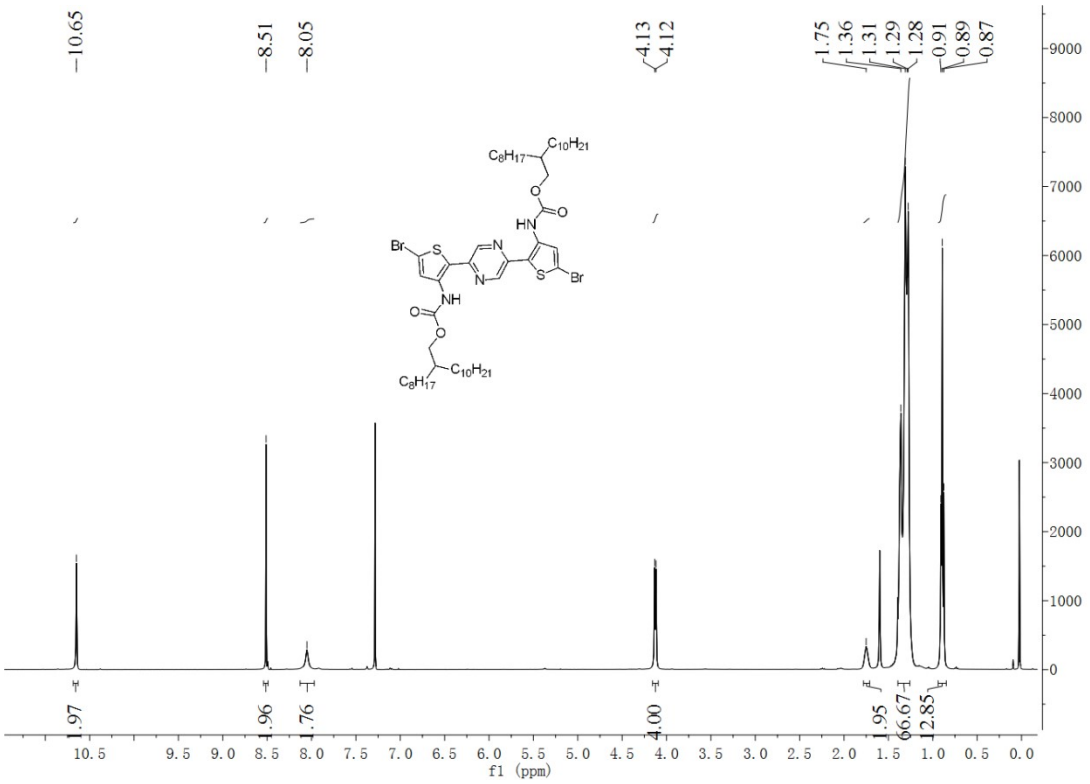

Figure S16. ^{1}H NMR spectrum of **7** in $CDCl_3$.

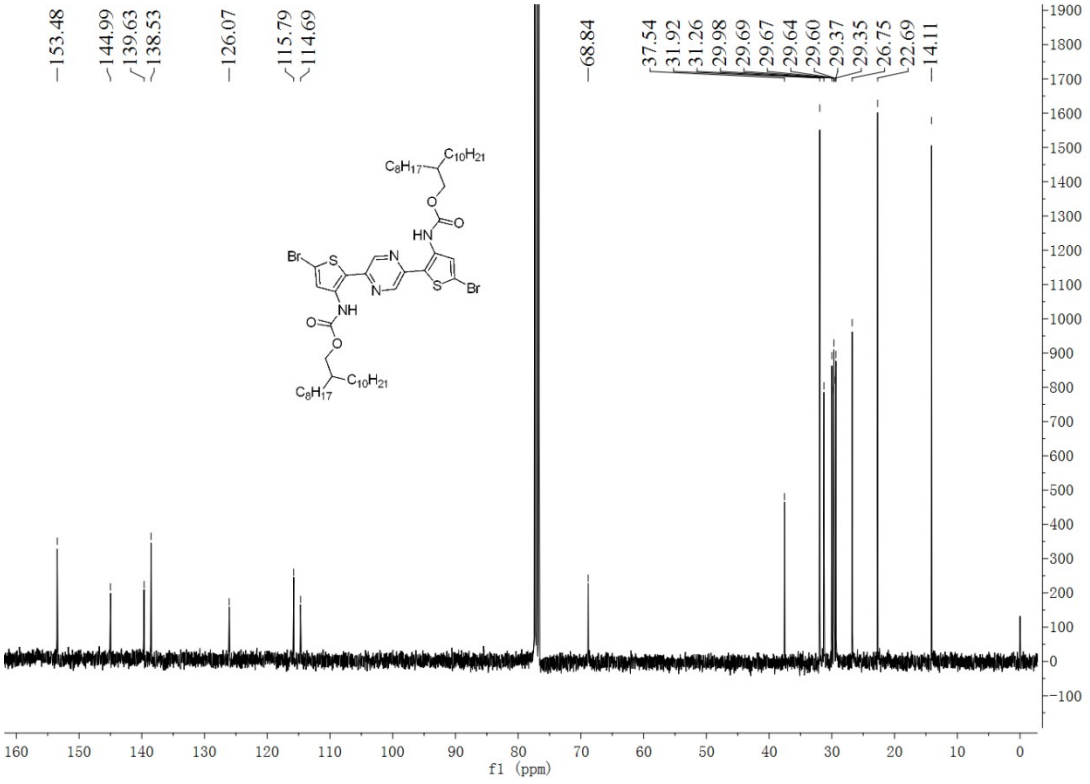

Figure S17. ^{13}C NMR spectrum of **7** in $CDCl_3$

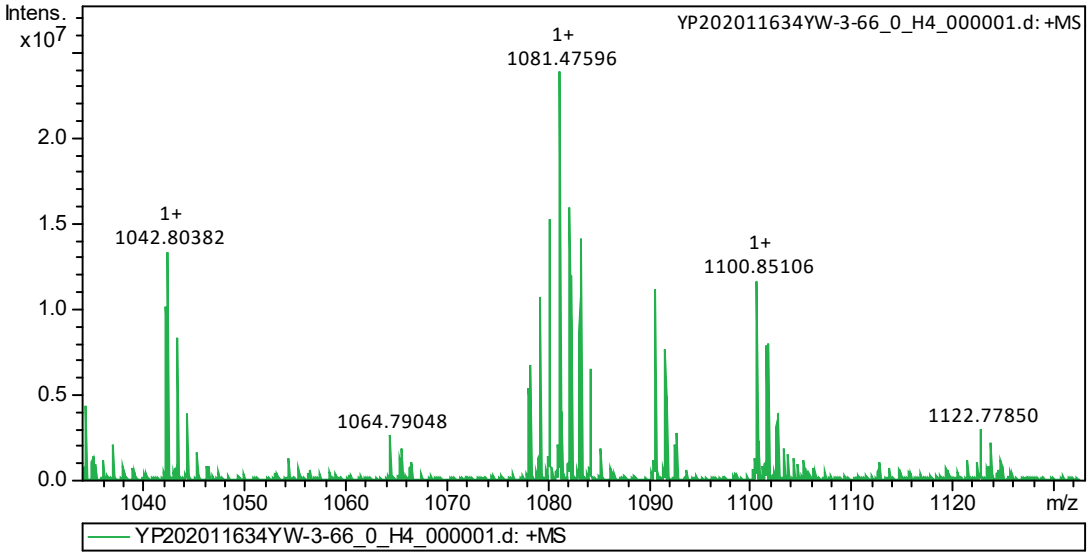

Figure S18. High-resolution MALDI-TOF MS spectrum of **7**

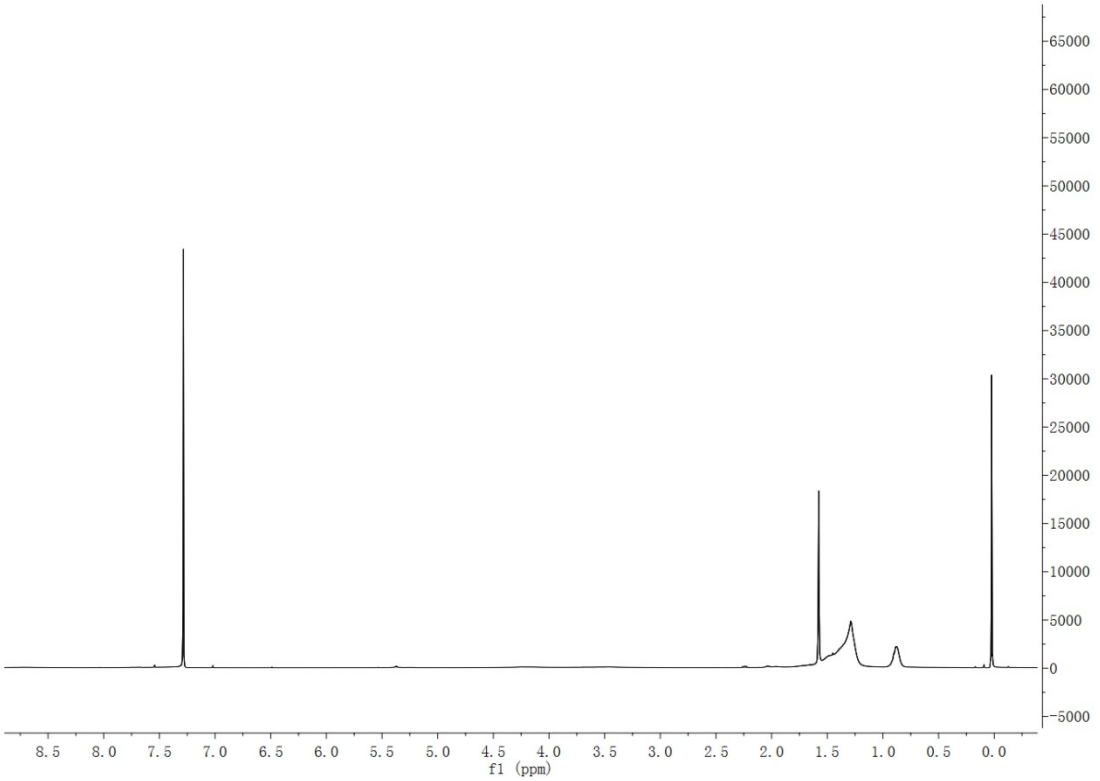

Figure S19. ^{1}H NMR spectrum of **PI-BDT1** in $CDCl_3$

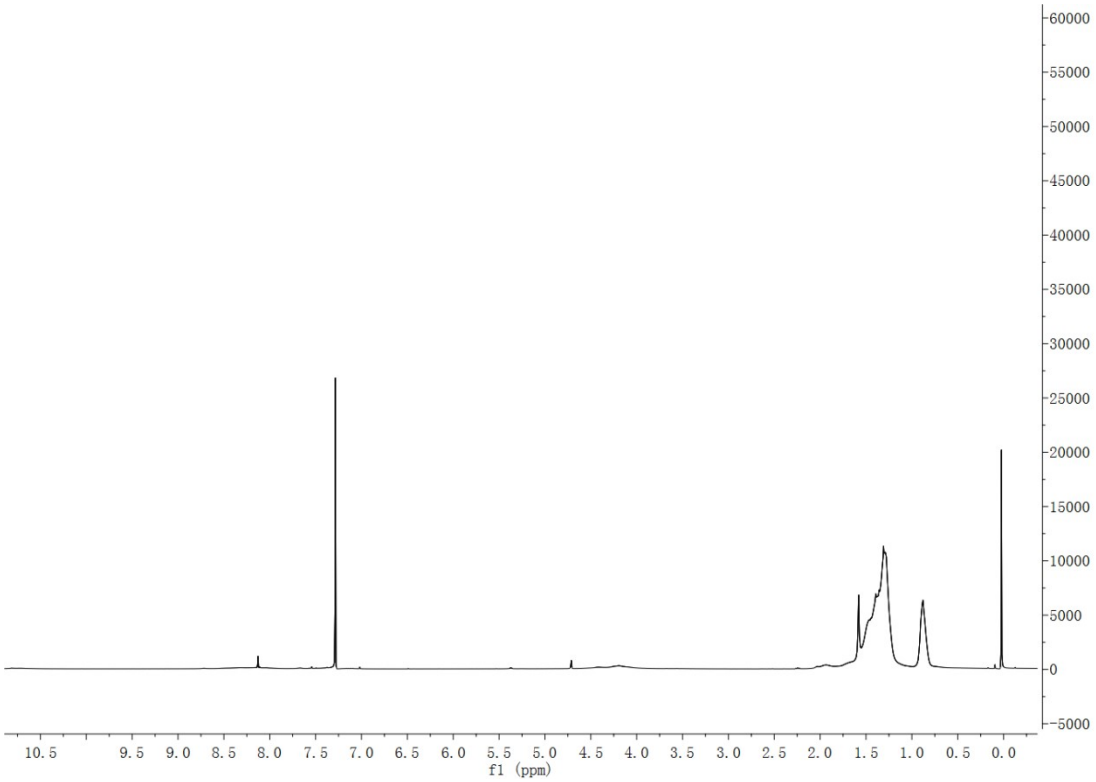

Figure S20. ^{1}H NMR spectrum of **PC-BDT1** in $CDCl_3$

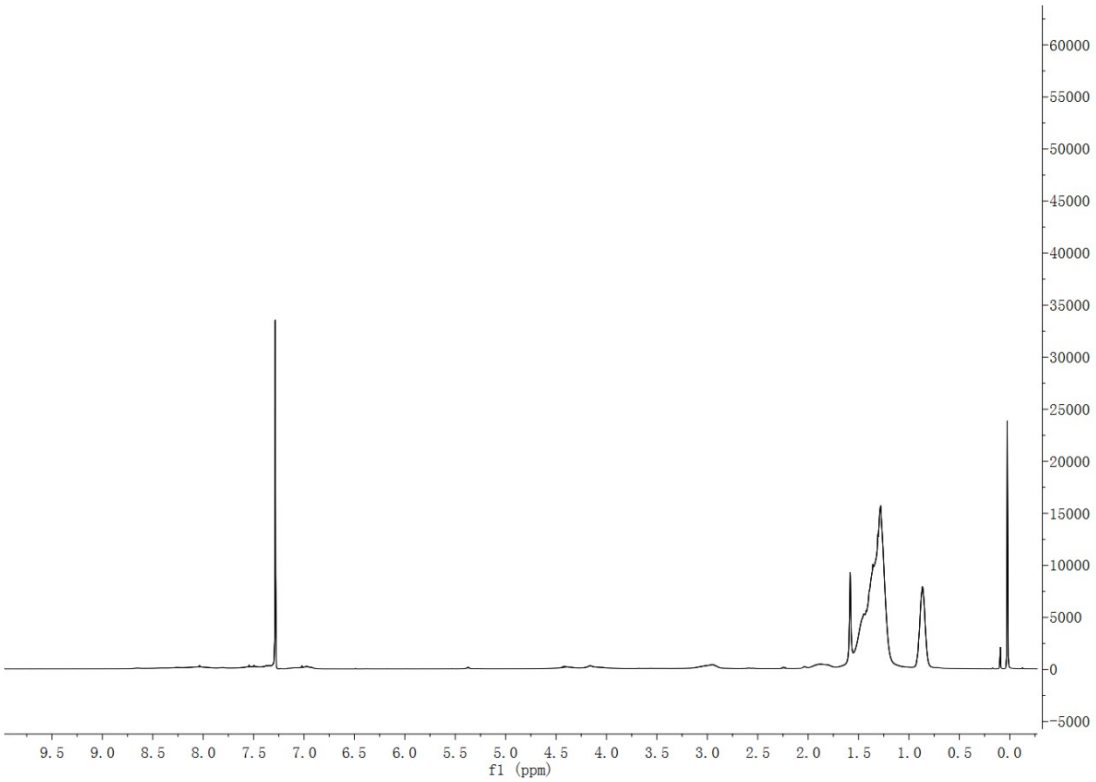

Figure S21. ^{1}H NMR spectrum of **PC-BDT2** in $CDCl_3$

2. Crystallographic Results

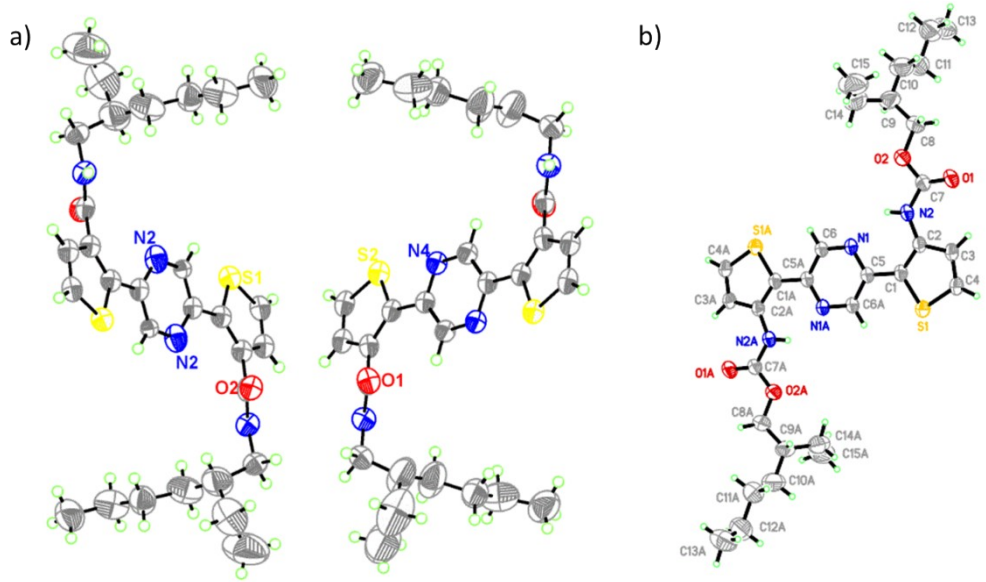

Figure S22. Single-crystal structures of complex **4a** (a) and **5a** (b)

Table S1. Crystal data and structure refinement for **4a**

Empirical formula	C60 H82 N8 O4 S4
Formula weight	1107.57
Temperature	173(2) K
Wavelength	1.54178 Å
Crystal system, space group	Triclinic, P $\bar{1}$
Unit cell dimensions	a = 5.1062(2) Å α = 82.251(2)°
	b = 15.6416(6) Å β = 89.811(2)°
	c = 18.7651(7) Å γ = 86.607(2)°
Volume	1482.45(10) $Å^3$
Z, Calculated density	1, 1.241 mg/m^3
Absorption coefficient	1.884 mm^{-1}
F(000)	594
Crystal size	0.160 x 0.150 x 0.120 mm
Theta range for data collection	2.376 to 71.822°.
Limiting indices	-6<=h<=6, -19<=k<=19, -23<=l<=22
Reflections collected / unique	34605 / 5689 [R(int) = 0.1195]
Completeness to theta	67.679 99.3 %
Refinement method	Full-matrix least-squares on F^2
Data / restraints / parameters	5689 / 1 / 351
Goodness-of-fit on F^2	1.022

Final R indices [I>2sigma(I)]	R1 = 0.1062, wR2 = 0.2796
R indices (all data)	R1 = 0.1537, wR2 = 0.3196
Extinction coefficient	n/a
Largest diff. peak and hole	0.934 and -0.628 e.A^{-3}

Table S2. Crystal data and structure refinement for **5a**

Empirical formula	C30 H42 N4 O4 S2
Formula weight	586.79
Temperature	297(2) K
Wavelength	1.54178 Å
Crystal system, space group	Triclinic, P ī
Unit cell dimensions	a = 5.1770(4) Å α = 100.491(4)°
	b = 10.4037(11) Å β = 97.244(4)°
	c = 15.1011(11) Å γ = 96.510(4)°
Volume	785.58(12) Å^3
Z, Calculated density	1, 1.240 mg/m^3
Absorption coefficient	1.885 mm^{-1}
F(000)	314
Crystal size	0.160 x 0.150 x 0.120 mm
Theta range for data collection	4.365 to 68.145°
Limiting indices	-6<=h<=6, -12<=k<=12, -18<=l<=18
Reflections collected / unique	11547 / 2855 [R(int) = 0.0446]
Completeness to theta	67.679 99.3 %
Refinement method	Full-matrix least-squares on F^2
Data / restraints / parameters	2855 / 1 / 187
Goodness-of-fit on F^2	1.356
Final R indices [I>2sigma(I)]	R1 = 0.0978, wR2 = 0.3007
R indices (all data)	R1 = 0.1086, wR2 = 0.3232
Extinction coefficient	n/a
Largest diff. peak and hole	0.545 and -0.357 e.A^{-3}

3. Thermal Analyses of Polymers

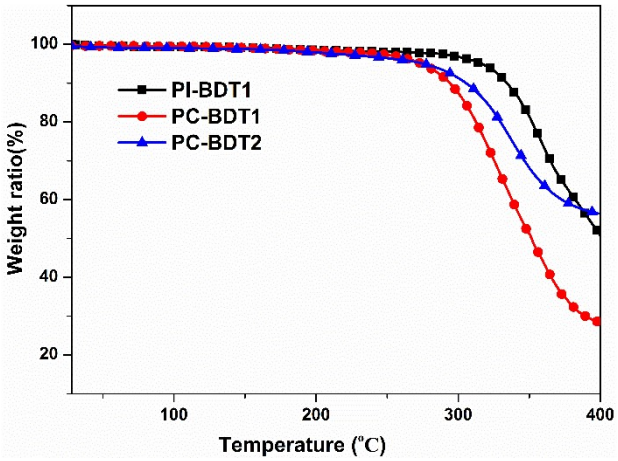

Figure S23. Thermogravimetric analysis (TGA) analysis of **PI-BDT1**, **PC-BDT1** and **PC-BDT2**.

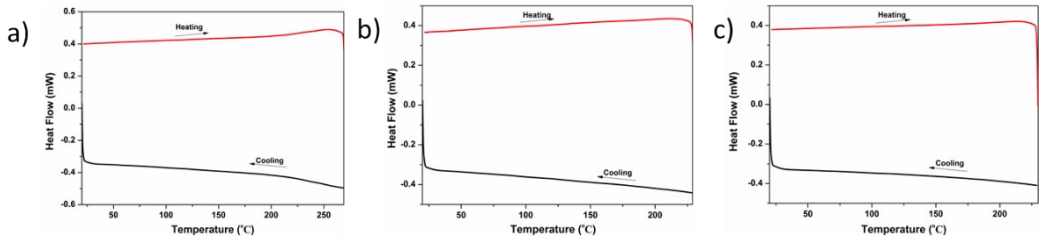

Figure S24. Differential scanning calorimetry (DSC) analysis of **PI-BDT1** (a), **PC-BDT1** (b) and **PC-BDT2** (c).

4. Ultraviolet photoelectron spectroscopy (UPS)

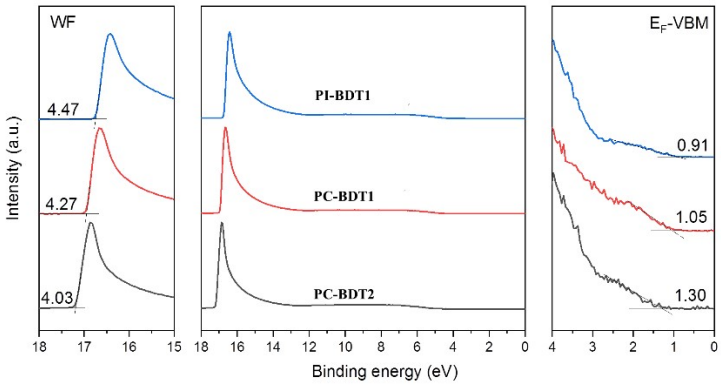

Figure S25. Ultraviolet photoelectron spectroscopy (UPS) of **PI-BDT1**, **PC-BDT1** and **PC-BDT2** thin films.

5. Photovoltaic Device Parameters

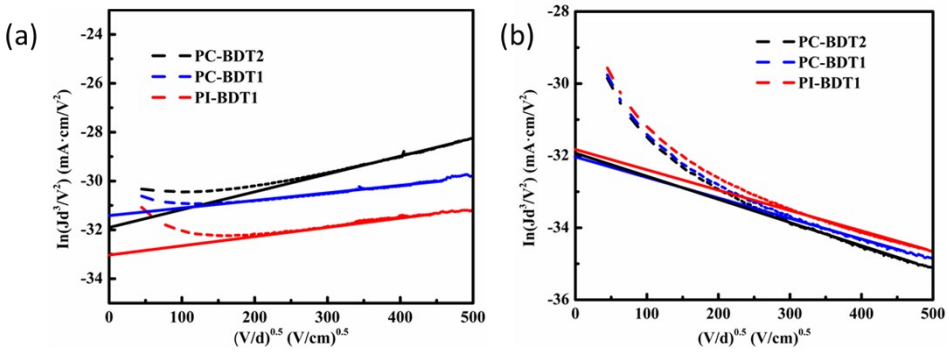

Figure S26. Characteristics of hole-only (a) and electron-only (b) devices for the measurement of the charge carrier transport in **PI-BDT1**, **PC-BDT1** and **PC-BDT2**:**Y6** blends by the SCLC method.

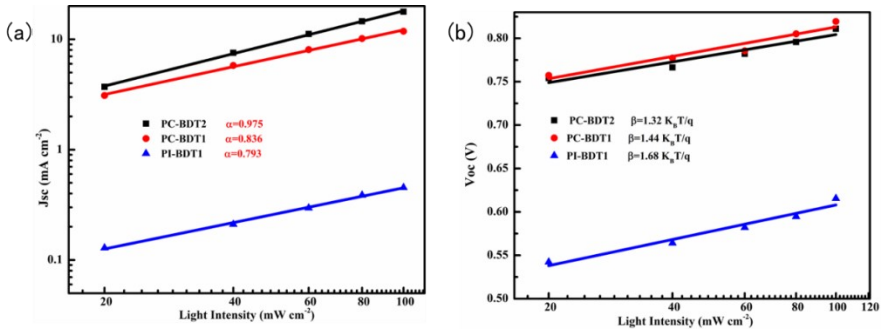

Figure S27. (a) Light intensity dependence of J_{SC} and (b) Light intensity dependence of V_{OC} of the solar cells.

6. Two-dimensional grazing incidence wide-angle X-ray scattering analysis

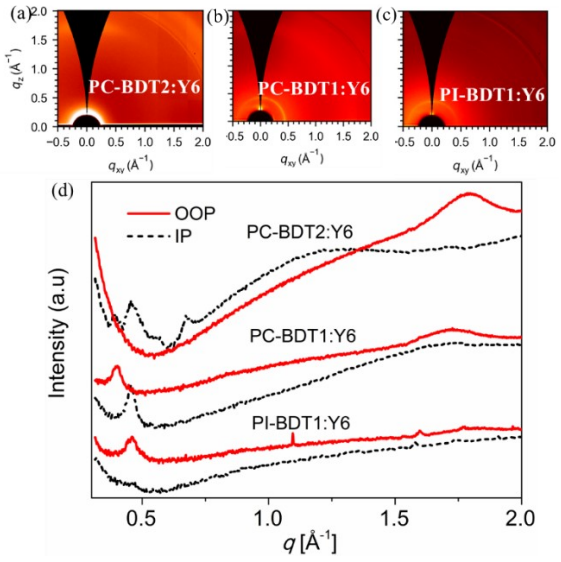

Figure S28. 2D GIWAXS patterns of the blend films (a) **PC-BDT2:Y6**, (b) **PC-BDT1:Y6,** (c) **PI-BDT1:Y6**, and (d) 1D GIWAXS profiles of corresponding blend

films along the out-of-plane (OOP, in red) and in-plane (IP, in black) directions.